Interpretation of the far-infrared spectrum of Fe^{2+} in cubic CdTe and ZnS

Eugenio E. Vogel* and Juan Rivera-Iratchet

Instituto de Física, Universidad de Concepción, Concepción, Chile

(Received 7 December 1979; revised manuscript received 14 April 1980)

The main purpose of this article is to report the result of calculations for the low-lying energy states of Fe^{2+} in CdTe. The analysis is extended to the fairly standard case of Fe^{2+} in ZnS as a verification of the method and to allow a more direct interpretation of the results. Special attention is paid to the relative energy of the levels, wave functions, and oscillator strengths for the far-infrared transitions. In doing so the crystalline field, spin-orbit interaction, spin-spin interaction, and Jahn-Teller effect are considered by means of perturbation theory and diagonalization of part of the Hamiltonian matrix. The results are found to be in satisfactory agreement with the available experimental information of optical absorption in the infrared and far-infrared spectrum. A comparison is also made with two previous different assignments for the optical transitions; our results are consistent with the earliest of these proposals. Effective values for crystal-field, spin-orbit, and Jahn-Teller parameters are calculated. The final eigenfunctions are tabulated.

I. INTRODUCTION

CdTe and ZnS crystallize in the fairly well-known zinc-blende structure. The atomic energy multiplets are then split by the crystalline field (CF) leading to new multiplets which can be furthter split by additional internal interactions such as spin-orbit (SO) and spin-spin interactions. In this way we would expect that the only difference between the spectrum of $CdTe:Fe^{2+}$ as compared to the one of $ZnS:Fe^{2+}$ would be due to the slightly different strength of the crystal fields. Moreover this difference would affect the splittings due to the internal interactions of the Fe^{2+} ion only as a second-order effect. Therefore one would expect that each line in the absorption spectrum of $ZnS:Fe^{2+}$ would have its counterpart in the spectrum of $CdTe:Fe^{2+}$ and vice versa, allowing for differences in the wavelengths of the absorbed radiation. In Fig. 1 we show schematically the splittings mentioned above showing the expected transitions due to both electric dipole and magnetic dipole absorptions at very low temperatures.

However, the experimental results to be discussed below show that the infrared lines of Fe^{2+} in CdTe are weaker than the corresponding lines for the same ion in ZnS. It is also found that the far-infrared absorption spectrum of $CdTe:Fe^{2+}$ is more complicated than the one for $ZnS:Fe^{2+}$, showing more absorption lines than those that can be expected from crystal-field theory. The explanation for this different behavior is to be found in the Jahn-Teller (JT) effect.[1] The larger masses of both Cd and Te atoms as compared with Zn and S, respectively, make possible that vibrational energies of the most abundant phonons are comparable to the energy differences between the electronic multiplets of Fe^{2+} in CdTe. In

this way the vibronic energy levels are almost degenerate in the adiabatic approximation, and even a weak JT coupling could be important for interpreting the spectrum. The lattice dynamics of both ZnS and CdTe have been studied by means of neutron scattering[2,3] and the results indeed show a larger number of lower-frequency modes for CdTe than for ZnS. It is one of the purposes of the present work to understand the differences in the optical properties of these two cases.

We summarize now the main experimental results that are relevant to the formulation of the model to be developed later.

a. $ZnS:Fe^{2+}$. The infrared absorption spectrum was determined by Slack, Ham, and Chrenko (SHC).[4] In this work the energy separation $10|Dq|$ between the $^5T_2$ and ^5E multiplets was reported to be about 3400 cm^{-1} and a first interpretation of the infrared spectrum was given. This spectrum was later reinterpreted by Ham and Slack[5] (HS) by taking into account the Jahn-Teller effect for the $^5T_2$ states that quenches the spin-orbit interaction. The most important transitions that are found at low temperatures are listed in Table I. The far-infrared spectrum has been determined by Slack, Roberts, and Ham[6] (SRH); the main absorption lines are presented in Table II. In addition this spectrum has also been studied in the presence of strong magnetic fields, allowing for a clear interpretation of the lines[7] in agreement with SRH. Also the lowest-energy interval between levels 1 and 2 of Fig. 1 show the expected Schottky anomaly in the heat capacity corresponding to a gap of about 15 cm^{-1}.[8]

b. $CdTe:Fe^{2+}$. The infrared absorption spectrum gives a value of approximately 2480 cm^{-1} for the crystal-field-splitting parameter $10|Dq|$.[4] A second
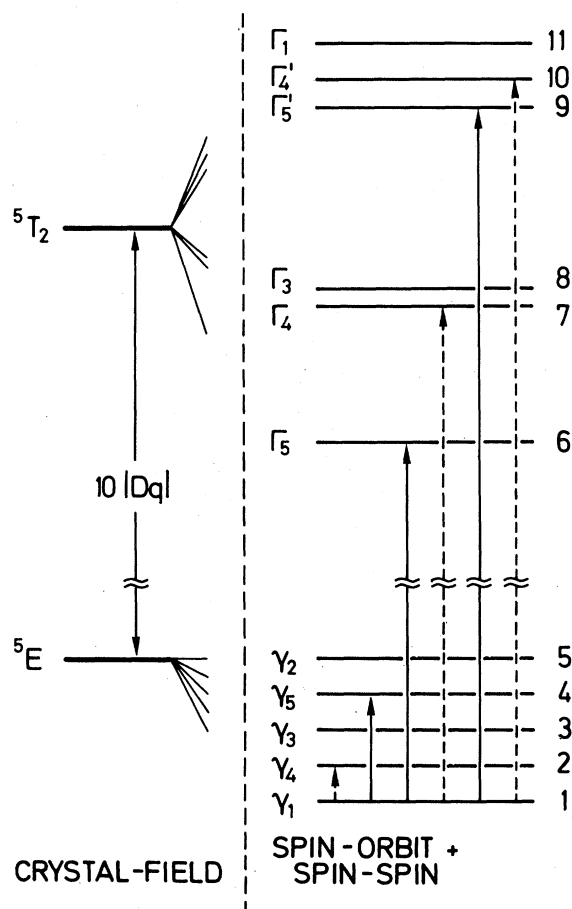
FIG. 1. Schematic of the energy-level splitting of the atomic ground multiplet ^5D of Fe^{2+} due to crystal-field and spin-orbit interaction. The resulting levels are labeled with the notation corresponding to the irreducible representations of the group Td. A sequential ordering with increasing energy is also given. The discontinuous and continuous arrows correspond to allowed magnetic dipole and electric dipole transitions, respectively.

determination of the spectrum followed by a critical review of the assignment of the lines was done by Slack, Roberts, and Vallin (SRV).[9] The most important absorption lines that are found at low temperatures are presented in Table I. The far-infrared spectrum was also determined by SRV[9] using magnetic fields to allow for a clearer identification of some of the transitions. The most important absorptions that are found in the far-infrared spectrum are listed in Table II.

Different calculations have been able to explain most of the experimental results summarized above. Thus, the close spacing of the energy levels coming from the $^5T_2$ multiplet (see Fig. 1 and Table I) has been explained as due to dynamical JT effects for the case of $ZnS:Fe^{2+}$.[5] It is expected that such an effect would be more pronounced in the case of $CdTe:Fe^{2+}$ due to the fact that the TA branch of the phonon dispersion curve for $CdTe^3$ has lower frequencies than the corresponding one for ZnS.[2] In this way more vibronic states can mix weakening the absorption rates as it is found experimentally (see Table I). We do not attempt here to calculate the JT effect for the $^5T_2$ states because of the too many assumptions about the modes, frequencies, and coupling parameters that would have to be made. Instead we recognize that such a JT effect would act as to quench the orbital operators for the electronic configuration of the impurity. We adopt then the approach of using adjustable parameters for the crystal-field and spin-orbit interaction. Thus we take the JT effect for the $^5T_2$ states into account indirectly and in a phenomenological context.

The far-infrared spectrum of $ZnS:Fe^{2+}$ can be interpreted in a straightforward way following SRH (Ref. 6) in what we will call "interpretation A" from now on. The low-temperature absorption lines encountered in the experiments are attributed to magnetic and dipole transitions in the way shown by Fig. 2(a). It seems the case that the JT effect for the ^5E levels of Fe^{2+} in ZnS is not significant enough to be

TABLE I. Low-temperature absorptions in the infrared spectra of $ZnS:Fe^{2+}$ and $CdTe:Fe^{2+}$ showing the energy E of the transitions (SHC, Ref. 4), the measured oscillator strengths (SHC, Ref. 4), and the assignments for the initial and final levels involved in the transition (HS, Ref. 5).

	$ZnS:Fe^{2+}$			$CdTe:Fe^{2+}$	
E (cm^{-1})	f (10^6)	Assignment[a]	E (cm^{-1})	f (10^6)	Assignment[a]
2947	50	(1–6)	2282	6	(1–6)
2966	2	(1–7)	2294	7	(1–7)
2986	0.5	(1–8)	2309	8	(1–8)

[a]According to Fig. 1 of this work.

TABLE II. Most important absorptions in the far-infrared spectra of ZnS:Fe^{2+} and CdTe:Fe^{2+} showing the energy E of the transitions, the measured oscillator strengths f, and the assignment for the different transitions. (For simplicity we do not report here the experimental error which can be found in the original articles.)

E (cm^{-1})	ZnS f (10^8)	Assignment[a]	E (cm^{-1})	CdTe f (10^8)	Assignment[a]
14.6[b]	0.7[b]	(1−2)[b]	18.6[c]	1.5[c]	(1−2)[c,d]
43.0[e]	⋯	Local[e]	36.0[c]	⋯	TA(L)[c,d]
			48.0[c]	⋯	TA(X)[c] (1−4)[d]
45.1[b]	4.0[b]	(1−4)[b]	66.7[c]	3.0[c] 1.5[d]	(1−4)[c] (1−2)[d]
			73.2[c]	3.0[c] 1.5[d]	(1−4)[c,d]
31.1[b,f]	0.3[b]	(2−4)[b]	54.8[c,f]	1.5[d]	(2−4)[c,d]

[a]According to Fig. 1 of this work.
[b]SRH, Ref. 6 (sample R 118).
[c]SRV, Ref. 9.

[d]Vallin, Ref. 10.
[e]VSB, Ref. 7.
[f]Transitions present at temperatures much larger than 4 K.

noticed in the absorption spectrum. On the other hand the necessity of considering the JT effect for the ^5E states of Fe^{2+} in CdTe was recognized in SRV, although no calculations along this line were reported. In Fig. 2(b) we represent the assignment proposed by SRV based on qualitative bases to explain the low-temperature absorption lines; this will be referred to as "interpretation B" from now on. The JT effect was considered for the ^5E states of Fe^{2+} in CdTe by Vallin[10] without taking into account the JT effect for the $^5T_2$ multiplet and diagonalizing the JT Hamiltonian with respect to a group of vibronic functions formed in the adiabatic limit. The low-temperature lines predicted by Vallin are shown in Fig. 2(c) in what we shall call "interpretation C." It is interesting to notice that in this interpretation it is
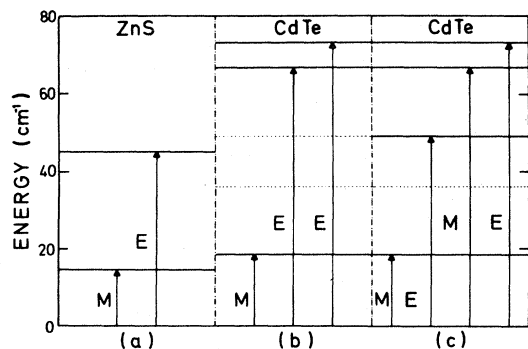

FIG. 2. Interpretations of the spectrum of Fe^{2+} in ZnS and CdTe at low temperatures. M and E are magnetic dipole and electric dipole transitions. (a) Reference 6, (b) Ref. 9, and (c) Ref. 10.

proposed that the already weak (1−2) magnetic dipole transtition would give rise to two magnetic dipole transitions at very different energies once the JT effect is considered. It is the main purpose of the present work to examine the case of Fe^{2+} in CdTe more carefully than done so far taking into account the JT effect for the $^5T_2$ multiplet in the way described above and to calculate the JT effect for the ^5E multiplet considering all the vibronic functions that are relevant in the calculation of the oscillator strengths. We perform the diagonalization of the crystal-field and spin-orbit interaction in the way presented in SRV, except that the parameters describing the interaction are now allowed to be quenched to explain a satisfactory adjustment of the infrared absorption spectra. We then include the JT effect in the way Vallin introduced it but the electronic functions are now different from those reported by SRV which were used as the starting point in the previous approach. We then calculate the oscillator strengths without neglecting a priori the contribution of some vibronic states as was apparently done before.[10] Our results for CdTe:Fe^{2+} are consistent with interpretation B which was proposed as a natural extension of interpretation A but there was no model calculation to support this proposal. As a consequence of these results the intriguing second absorption line associated with magnetic dipole transitions proposed in interpretation C is not possible at all.

The eigenfunctions corresponding to the low-energy states of the two systems are listed to allow for applications of the present results to other problems. It would be of particular interest, for instance, to attempt a calculation of the thermal conductivity

of CdTe:Fe^{2+} due to resonant scattering of phonons by the electronic structure of the impurity.[11,12]

Although the results of our calculations do not modify the present understanding of the absorption spectra of ZnS:Fe^{2+} we maintain this case in parallel to the one of CdTe:Fe^{2+}. The simplicity of the far-infrared spectrum of the former will allow us to check the general method and to draw the final conclusions. However, the emphasis of the presentation is on CdTe:Fe^{2+}.

We have divided this article in six sections. In Sec. II we include a very brief presentation of the crystal-field Hamiltonian. In Sec. III we present the treatment of the spin-orbit interaction. In Sec. IV the JT effect for the ^5E multiplet is introduced and the final wave functions are reported. Section V is devoted to the calculation of the oscillator strengths for the different transitions. In Sec. VI the results are discussed and the main conclusions are given.

II. CRYSTAL FIELD

The lowest-energy level of the free ion Fe^{2+} is ^5D as can be found by direct application of Hund's rules. The Hamiltonian for the CF in cubic symmetry of tetrahedral coordination[13] reduces to the form

$$V(r, \Theta, \phi) = r^4(B_0^4 C_0^{(4)} + B_4^4 C_4^4 + B_{-4}^4 C_{-4}^{(4)}) , \quad (1)$$

where r, θ, and ϕ are spherical coordinates that describe the position of a d electron with respect to an origin fixed at the center of the iron nucleus. B_l^m is a coefficient of the expansion. $C_l^{(m)}(\theta, \phi)$ is a spherical tensor related to the spherical harmonics.

The 25 electronic states can be labeled by using the basis functions of the representations of the group T_d. Since $S = L = 2$ in the ion, we can make use of the reduction of the representation D^2 of the group R (3) with respect to the representations of the group T_d:

$$D^2 \rightarrow E + T_2 .$$

By means of angular momentum techniques[14] we can calculate the splitting of the free ion's ground level due to the crystal field. The results of such a calculation show that there are two multiplets: the upper one has orbital symmetry T_2 with total degeneracy of 15; the lower one has orbital symmetry E with total degeneracy of 10. This is shown in the left-hand side of Fig. 1.

The five spin functions can now be labeled as θ, ϵ, x, y, z.[15] Exactly the same can be done with the five orbital functions. The 25 electronic functions will be denoted as $|ij\rangle$ where both i and j run independently over θ, ϵ, x, y, and z. We follow the convention that the first symbol in the ket denotes spin symmetry while the second one denotes orbital symmetry.

With this notation the 15 states of the upper mul-

tiplet can be written as $|ix\rangle$, $|iy\rangle$, and $|iz\rangle$, while the 10 states of the lower multiplet can be written as $|i\theta\rangle$ and $|i\epsilon\rangle$, where i runs over the five independent spin functions.

III. SPIN-ORBIT INTERACTION

The Hamiltonian of the SO interaction has the form

$$H_{SO} = \lambda \vec{S} \cdot \vec{L} , \quad (2)$$

where λ depends on the properties of the radial wave functions of the atomic multiplet of Fe^{2+}. For the free ion[16] $|\lambda| = 100 \pm 10$ cm^{-1}. $\vec{S}$ and $\vec{L}$ represent the total spin and angular orbital momentum, respectively.

The electronic functions can be symmetrized so that the new set transforms as basis functions for the irreducible representations of T_d. The 10 functions of the lower multiplet are given in Table III while the 15 functions of the upper multiplet are given in Table IV.

The matrix elements of the total Hamiltonian (CF plus SO) are calculated by means of representation of the $\vec{S}$ and $\vec{L}$ operators[17] with respect to the spin and orbital functions, respectively. The results agree very well with SRV.[9] The only difference is that our functions are defined in terms of the basis functions of the group T_d instead of using angular momentum functions as in the previous work. Since our final calculation includes JT effects it is advantageous to formulate the problem in terms of the point symmetry at the crystal site.

Let us summarize here the main general results.

(a) It is found that diagonalization of the matrix should be used to obtain more exact values.[9]

(b) The ground multiplet splits into five levels: γ_1, γ_4, γ_3, γ_5, and γ_2 (the listing is given in terms of increasing energy). The upper multiplet splits into six levels which can be ordered in the following way in terms of increasing energy: Γ_5, Γ_4, Γ_3, Γ'_5, Γ'_4, and Γ_1.[15] These eleven levels will be identified by the numbers 1,2, . . . , 11 in order of increasing energy whenever we refer to them (see Fig. 1.).

(c) Absorptions from the two lowest levels to the upper ones are possible according to Table V.

The results for each compound will now be discussed bearing in mind the three interpretations shown in Fig. 2.

a. ZnS. When the values $\lambda = -100$ and $Dq = -340$ are used in the diagonalization process the energies of the eleven levels are the following: 0.0, 14.7, 29.5, 47.3, 65.5; 3177, 3382, 3401, 3672, 3700, and 3731. The energies can be varied by letting λ take different values. In this way the absorption at 14.6 and 45.1 cm^{-1} can be explained. However, there is no way to explain the line at 2947 cm^{-1} and

TABLE III. Eigenfunctions of the 10 states belonging to the lower electronic multiplet. N denotes the normalization factor $(g=\sqrt{3})$.

Irr. rep.	Function	N^2	$|\theta\theta\rangle$	$|\epsilon\theta\rangle$	$|x\theta\rangle$	$|v\theta\rangle$	$|z\theta\rangle$	$|\theta\epsilon\rangle$	$|\epsilon\epsilon\rangle$	$|x\epsilon\rangle$	$|v\epsilon\rangle$	$|z\epsilon\rangle$
γ_2	$|b\rangle$	2		−1				1				
	$|x\rangle$	4			−1					g		
γ_5	$|y\rangle$	4				−1					$-g$	
	$|z\rangle$	1					1					
	$|\theta\rangle$	2	−1						1			
γ_3	$|\epsilon\rangle$	2		1				1				
	$|u\rangle$	4			$-g$					−1		
γ_4	$|v\rangle$	4				g					−1	
	$|w\rangle$	1										1
γ_1	$|a\rangle$	2	1						1			

others very close to this one unless $|Dq|$ and $|\gamma|$ are reduced.

b. CdTe. For $\lambda = -100$ and $Dq = -248$ we find, after diagonalizing the Hamiltonian, the following energies: 0.0, 18.6, 37.3, 61.5, 86.7; 2281.8, 2487.9, 2516.2, 2775.9, 2813.7, and 2853.5. Again the energies of levels 2 and 4 can be adjusted to get partial agreement with the experiment by means of either interpretation *B* or *C*. However, we still find that the levels originating from the upper multiplet are too spread out to be consistent with the interpretation of the infrared spectrum.[4]

The experimental evidence shows that the levels that originate from the upper multiplet are much less spread out than predicted by the calculations described above. On the other hand the "center of gravity" of the upper multiplet seems to be decreased in energy. At least two causes can be proposed to explain these deviations from simple crystal-field calculations: (1) The mixing of the lowest atomic multiplet with some of the nearest excited atomic multiplets. However one can expect that such corrections would contribute a few cm^{-1} at the most. (2) The ultimate reason seems to be in the dynamical JT effect that will act on the states of the upper multiplet.

It is almost impossible at the moment to perform *ab initio* calculations of the actual quenching factors for the states of the upper multiplet. There are two vibrational modes E and six vibrational modes T_2 for the tetrahedron. This means that three vibrational frequencies are unknown. The linear coupling constants between the electronic system and each of the

TABLE IV. Eigenfunctions of the 15 states belonging to the upper electronic multiplet. N denotes the normalization factor $(g=\sqrt{3})$.

Irr. rep.	Function	N^2	$|\theta x\rangle$	$|\epsilon x\rangle$	$|xx\rangle$	$|yx\rangle$	$|zx\rangle$	$|\theta y\rangle$	$|\epsilon y\rangle$	$|xy\rangle$	$|yy\rangle$	$|zy\rangle$	$|\theta z\rangle$	$|\epsilon z\rangle$	$|xz\rangle$	$|yz\rangle$	$|zz\rangle$
Γ_1	$|A\rangle$	3			1						1						1
	$|U'\rangle$	12	g	−1								−2				2	
Γ_4'	$|V'\rangle$	12						2	$-g$	1					−2		
	$|W'\rangle$	3				−1						1			−1		
	$|X'\rangle$	20	g	−3								2				2	
Γ_5'	$|Y'\rangle$	20						2	g	−3					2		
	$|Z'\rangle$	5					1			1			$-g$				
	$|\Theta\rangle$	6			−1						−1						2
	$|E\rangle$	2			1						−1						
	$|U\rangle$	6	$-g$	−1								−1				1	
Γ_4	$|V\rangle$	6						1	g	−1					−1		
	$|W\rangle$	6		−1								1			2		
	$|X\rangle$	10	−1	g									g			g	
Γ_5	$|Y\rangle$	10						g	−1	$-g$					g		
	$|Z\rangle$	10					g			g		2					

TABLE V. Allowed absorptions originating from the two lowest levels after spin-orbit interactions. E: electric dipole transition; M: magnetic dipole transition; 0: no dipole transition. This table is applicable to Fe^{2+} in both CdTe and ZnS.

Level	Irr. rep.	Type of absorptions initial level: γ_1	γ_4
11	Γ_1	0	M
10	Γ_4'	M	$E+M$
9	Γ_5'	E	$E+M$
8	Γ_3	0	M
7	Γ_4	M	$E+M$
6	Γ_5	E	$E+M$
5	γ_2	0	E
4	γ_5	E	$E+M$
3	γ_3	0	$E+M$
2	γ_4	M	$\cdots$
1	γ_1	$\cdots$	$\cdots$

three vibrational energies are also unknown. Although several assumptions can be made in order to get an understanding of the JT effect in the upper multiplet, such an approach is not within the scope of the present article. We simply assume that the Jahn-Teller effect will act strongly on levels Γ_4, Γ_4', Γ_5, and Γ_5' because there are many vibronic levels with symmetries Γ_4 and Γ_5 so the mixing of the zero-quantum states with one-quantum states will be pronounced. As a matter of fact, one has to form 10×10 matrices to study the linear JT coupling that affects the zero-quantum states Γ_4 or Γ_5 (considering only one phonon). As a result of this analysis one should get large reductions of the spin-orbit corrections for states of Γ_4 or Γ_5 symmetry. The quenching factors are not so pronounced for the state Γ_1 as in

the case of Γ_4 and Γ_5 states. A 4×4 matrix will be enough to include all those one-quantum vibronic levels that couple directly to the zero-quantum state.

Now we make two assumptions in order to get some understanding of the splitting of the lower multiplet. In the first place, we assume that the separation Δ between the two multiplets is less than $10|Dq|$; this is due to the JT effect. We define an "effective $|Dq|$" (denoted by D) which can be adjusted so as to give the absorption connecting the levels γ_1 and Γ_5 (1 and 6). In the second place, we assume that the quenching of the SO interaction is total for states of symmetry Γ_4 or Γ_5 in the upper multiplet.

The quenching of the spin-orbit interaction for the state Γ_1 is taken as partial. Its value can be obtained by adjustment of the calculations for the γ_1 to γ_4 transition (1 to 2). The quenching of the SO interaction for the states of Γ_3—although it should be intermediate between the two previous cases (the mixing is now described by a 6×6 matrix)—will be taken as total since there is not experimental information to clearly identify the location of the γ_3 and Γ_3 levels.

With the assumptions described above we can reformulate the diagonalization of the SO matrices due to the SO interaction. It is also possible to incorporate the weak spin-spin interaction that is also present. Such a Hamiltonian within an atomic multiplet[18] of common spin and orbital angular momenta can be written as

$$H_{SS} = -\rho[(\vec{S}\cdot\vec{L})^2 + \tfrac{1}{2}(\vec{S}\cdot\vec{L})] , \qquad (3)$$

where $\vec{S}$ and $\vec{L}$ play the role of dimensionless operators isomorphic to spin and orbital angular momentum operators, respectively. The factor ρ gives the magnitude of the interaction; its theoretical value[18] is 0.18 cm^{-1}.

We give now one typical matrix for each irreducible representation of the group T_d:

$$A; \quad \begin{array}{c} a \\ A \end{array} \begin{vmatrix} -6D-24\rho & f(2x-3\rho) \\ f(2x-3\rho) & 4D+2xR_a-27\rho \end{vmatrix} ,$$

$$E; \quad \begin{array}{c} \theta \\ \Theta \end{array} \begin{vmatrix} -6D-12\rho & g(2x+3\rho) \\ g(2x+3\rho) & 4D-xR_e-13.5\rho \end{vmatrix} ,$$

$$T_1; \quad \begin{array}{c} w \\ W \\ W' \end{array} \begin{vmatrix} -6D-18\rho & -f(x+15\rho) & g(2x-3\rho) \\ -f(x+1.5\rho) & 4D-xR_1-7.5\rho & 0 \\ g(2x-3\rho) & 0 & 4D+2xR_1'-15\rho \end{vmatrix} ,$$

$$T_2; \quad \begin{array}{c} z \\ Z \\ Z' \end{array} \begin{vmatrix} -6D-6\rho & -p(6x+21\rho) & -q(2x-3\rho) \\ -p(6x+21\rho) & 4D-3xR_2-14.1\rho & 0 \\ -q(2x-3\rho) & 0 & 4D+2xR_2'-5.4\rho \end{vmatrix} ,$$

where $f = \sqrt{6}$, $g = \sqrt{3}$, $p = \sqrt{0.1}$, $q = \sqrt{0.6}$, $x = |\lambda|$, and D represents the absolute value of the effective Dq.

The quenching of the SO interaction within the upper multiplet is taken into account by means of the reduction factors R_a, R_e, R_1, R_1', R_2, and R_2'. These reduction factors are defined as the ratio of the effective spin-orbit coupling constant with respect to the free ion coupling constant. The matrices above are very general. In particular, if we make $D = |D_q|$, $x = 100$, $\rho = 0$, and $R_a = R_e = R_1 = R_1' = R_2 = R_2' = 1$, we obtain the numerical results that were discussed above.

The contribution of the spin-spin interaction to the splitting of the levels of the lower multiplet is hard to separate from the splitting caused by the spin-orbit interaction. We found that it is possible to adjust the energies of the lower levels using continuous values of x and ρ. Since the theoretical value of ρ is so small, we just neglect the spin-spin interaction in the face of CF and/or SO coupling constants. The effect of this is that the value of x that fits the energies of the lower multiplet will be somewhat larger than the true spin-orbit coupling parameter.

The quenching of the orbital operators for states of the upper multiplet is considered next. According to the way that was described above this can be done by simply making $R_e = R_1 = R_1' = R_2 = R_2' = 0.0$ while R_a is taken as an adjustable parameter.

Now we are ready to diagonalize the matrices with three parameters to be varied: D, x, and R_a. It is found that D is fixed by adjusting the absorption line between levels 1 and 6. The value of x is determined fundamentally by adjusting the hot line between levels 2 and 4. The value of R_a affects the energy of the ground state so it can be obtained by adjusting the absorptions between levels 1 and 2. In this way

this is not a random adjustment of energy levels with three parameters but rather a directed adjustment by taking into account the relative importance of each parameter. An iterative procedure is necessary in any case.

We now give the results of the adjustment for each compound.

a. ZnS. It was found that the best set of parameters that gives good results is: $D = 289$ cm^{-1}, $x = 87$ cm^{-1}, and $R_a = 0.15$. Then the energies of the levels 1 through 11 are the following: 0.0, 14.5, 29.9, 45.3, 60.9, 2951, 2951, 2982, 2967, 2997, and 3042 cm^{-1}. The agreement with the experimentally observed absorptions[4,6] at low temperatures is very good. The allowed transitions identified by the experiments are 14.6, 45.1, 2947, 2966, and 2986 cm^{-1} (the experimental error is omitted). The hot line experimentally determined at 31.1 cm^{-1} is also consistent with a transition between levels 2 and 4 at 30.8 cm^{-1}. The theoretical hot line between levels 2 and 5 at 46.4 cm^{-1} would be masked by the strong cold line at 45.3 cm^{-1} and by the presence of the local mode at 43 cm^{-1}.[7] The rest of the possible transitions between levels of the lower multiplet are either small or forbidden by selection rules. These points will be made more clear when discussing the oscillator strengths for the transitions, in Sec. V.

It is interesting to form the ratios between the actual parameters used in the adjustment and those determined when the quenching factors do not play an important role ($|Dq| = 340$ cm^{-1} and $|\lambda| = 100$ cm^{-1}).

$$D/|Dq| = 0.85; \quad x/|\lambda| = 0.87; \quad R_a = 0.15 . \quad (4)$$

b. CdTe. In this case the best set of parameters that give good results are $D = 219$ cm^{-1}, $x = 99$, and $R_a = 0.75$. The energies of levels 1 through 11 come

TABLE VI. General expression for typical eigenfunctions after spin-orbit interaction for the lower multiplet of Fe^{2+} in both CdTe and ZnS. The energies of the levels are also given for the best values found in the adjustment.

Irr. rep.	Symbol	General expression	Energies (cm^{-1}) CdTe	ZnS
γ_2	$|b\rangle$	$c_2|b\rangle$	96.5	60.9
γ_5	$|z\rangle$	$c_5|z\rangle + \delta_5|Z\rangle + \delta_5'|Z'\rangle$	70.0	45.3
γ_3	$|\theta\rangle$	$c_3|\theta\rangle + \delta_3|\Theta\rangle$	44.1	29.9
γ_4	$|w\rangle$	$c_4|w\rangle + \delta_4|W\rangle + \delta_4'|W'\rangle$	18.8	14.5
γ_1	$|a\rangle$	$c_1|a\rangle + \delta_1|A\rangle$	0.0	0.0
Effective $|Dq|$ (cm^{-1})			219	289
Spin-orbit parameter (cm^{-1})			99	87
Reduction factor for state Γ_1			0.75	0.15

TABLE VII. Coefficients for the eigenfunctions belonging to the lower multiplet of Fe^{2+} in both CdTe and ZnS. The evaluation was performed with the parameters that give the best adjustment of the energy levels.

Irr. rep	i	CdTe c_i	δ_i	δ_i'	ZnS c_i	δ_i	δ_i'
γ_2	2	+1.0000			+1.0000		
γ_5	5	+0.9941	+0.0842	+0.00688	+0.9973	+0.0567	+0.00463
γ_3	3	+0.9885	−0.1512		+0.0047	−0.1026	
γ_4	4	+0.9833	+0.1051	−0.1487	+0.9922	+0.0720	−0.1018
γ_1	1	+0.9808	−0.1952		+0.9899	−0.1415	

out to be: 0.0, 18.8, 44.1, 70.0, 96.5; 2286, 2286, 2339, 2313, 2364, and 2533 cm^{-1}. The agreement with the experimental results[4,9] is satisfactory within the framework of interpretation B. The allowed transitions would then be 18.6, 67.6, 73.2, 2282, 2294, and 2309 cm^{-1}. According to interpretation B the theoretical line at 70 cm^{-1} splits into two lines of comparable intensities. Then the lines at 66.7 and 73.2 cm^{-1} can be explained by the presence of a weak Jahn-Teller coupling that would remove a degeneracy of vibronic states. The hot line at 54.8 cm^{-1} would correspond to a transition from the level with energy 18.8 cm^{-1} to the level at about 73.2 cm^{-1}. The high-temperature transition between the levels at 18.8 cm^{-1} and 67.6 cm^{-1} would be masked by the absorption lines of the local modes. (This would contribute to the structure of the high-temperature spectrum from 40 to 50 cm^{-1}.) The ratios between the quenched and unquenched parameters are now the following ($|Dq| = 248$ cm^{-1} and $|\lambda| = 100$ cm^{-1}):

$$D/|Dq| = 0.88; \quad x/|\lambda| = 0.99; \quad R_a = 0.75 \quad . \tag{5}$$

The results for ZnS show that no further interactions need to be included to explain the spectrum of Fe^{2+}. However, in the case of Fe^{2+} in CdTe there is evidence of the existence of in-band resonant modes with energies comparable to the energies of the electronic state. Then, some of the vibronic states can be degenerate and even a small JT coupling can shift the zero-phonon states appreciably. The eigenfunctions and energies of the different states of the lower multiplet are given in Table VI for both Fe^{2+}:CdTe and Fe^{2+}:ZnS. The parameters that give the best adjustment of the energy levels are then used to evaluate the coefficients in the eigenfunctions. These coefficients are tabulated in Table VII.

IV. JAHN-TELLER EFFECT

The local modes corresponding to the vibrations of the tetrahedron can be classified according to the irreducible representations of the group T_d. The following normal modes are readily found[19]: A_1, E, T_1, and $2T_2$. The only modes that would couple to the E orbital electronic states of the lower multiplet are A_1 and E. The so-called breathing mode does not modify the spectrum. The two modes corresponding to the E representation will be designated by Θ and ϵ.

The vibrational Hamiltonian has the form

$$H_v = \hbar\omega(a_\Theta^\dagger a_\Theta + a_\epsilon^\dagger a_\epsilon + 1) \quad , \tag{6}$$

where $\hbar\omega$ is the vibrational energy for modes E. The creation $(a^\dagger)$ and annihilation (a) operators satisfy the usual commutation relations.[20] The normalized eigenfunctions of H_v will be denoted by $|nm\rangle$, where n is the Θ quantum number while m is the ϵ quantum number. The following properties are often used in the calculations

$$a_\Theta^\dagger|nm\rangle = (n+1)^{1/2}|n+1\,m\rangle, \quad a_\epsilon^\dagger|nm\rangle = (m+1)^{1/2}|n\,m+1\rangle \quad ,$$

$$a_\Theta|nm\rangle = n^{1/2}|n-1\,m\rangle, \quad a_\epsilon|nm\rangle = m^{1/2}|n\,m-1\rangle \quad . \tag{7}$$

The zero-order vibronic functions in the limit of weak JT effect can be formed by combinations of products of vibrational and electronic functions. In doing so we follow closely the work by Vallin.[10]

The product wave functions will be denoted as $|e,nm\rangle$, where e represents the electronic function while nm represents the vibrational function. The actual vibronic functions (with specific symmetry properties) will be denoted as $|(rN)s\rangle$, where r represents the original electronic representation, N represents the total quantum vibrational number $(N = n + m)$, and s is one of the symbols that corresponds to a

basis function of the irreducible representations of the group T_d. In defining the vibronic functions we neglect the mixing with the upper multiplet due to SO interaction. The most important zero-order vibronic functions are listed in Table VIII.

The Hamiltonian for the JT effect can be written in the form[21]

$$H_{JT} = K[(a_\Theta^\dagger + a_\Theta)D_\Theta + (a_\epsilon^\dagger + a_\epsilon)D_\epsilon] ,   (8)$$

where D_Θ and D_ϵ are dimensionless operators that act on the orbital coordinates of the electron. K plays the role of a coupling constant for the JT effect in such a way that the JT energy is given by

$$E_{JT} = K^2/\hbar\omega .$$

The matrix representation of the operators D_Θ and D_ϵ on a base formed by orbital Θ and ϵ functions are the following[17]:

$$D_\Theta = \begin{vmatrix} -1 & 0 \\ 0 & +1 \end{vmatrix}; \quad D_\epsilon = \begin{vmatrix} 0 & 1 \\ 1 & 0 \end{vmatrix} .   (9)$$

By using Eqs. (6)–(9) we can calculate the matrix element of the Hamiltonian

$$H' = H_v + H_{JT}   (10)$$

with respect to the zero-order vibronic functions given in Table VIII.

The spectrum of Fe^{2+} in ZnS is well explained by the spin-orbit interaction. We make the assumption

TABLE VIII. Zero-order vibronic eigenfunctions. The product of the electronic and vibrational functions is denoted by $|e,nm\rangle$. The zero-order vibronic eigenfunction is denoted by $|(rN)s\rangle$ identifying the irreducible representation of the electronic part r, the total number of vibrational quanta N, and the isomorphic basis function of the group T_d. $(a = 1/\sqrt{2}.)$

Zero-order vibronic	Expression
$|(20)b\rangle$	$|b, 00\rangle$
$|(31)b\rangle$	$a|\theta, 01\rangle - a|\epsilon, 10\rangle$
$|(51)z\rangle$	$|z, 10\rangle$
$|(50)z\rangle$	$|z, 00\rangle$
$|(42)z\rangle$	$|w, 11\rangle$
$|(41)z\rangle$	$|w, 01\rangle$
$|(51)w\rangle$	$|z, 01\rangle$
$|(42)w^b\rangle$	$a|w, 20\rangle + a|w, 02\rangle$
$|(42)w^a\rangle$	$-a|w, 20\rangle + a|w, 02\rangle$
$|(41)w\rangle$	$|w, 10\rangle$
$|(40)w\rangle$	$|w, 00\rangle$
$|(30)\theta\rangle$	$|\theta, 00\rangle$
$|(11)\theta\rangle$	$|a, 10\rangle$
$|(31)a\rangle$	$a|\theta, 10\rangle + a|\epsilon, 01\rangle$
$|(10)a\rangle$	$|a, 00\rangle$

that there is no Jahn-Teller effect that will show up in the far-infrared spectrum of Fe^{2+} in ZnS. This can be due to two main reasons. One is that the JT coupling with E orbital states is rather weak for Fe^{2+} in ZnS, CdTe, and other compounds of the same crystal structure. The other reason is that in-band resonant modes of Fe^{2+} in ZnS have higher frequencies than those of Fe^{2+} in CdTe so the degeneracy that is present in the latter (see below) is not present in the former.

In the case of Fe^{2+} in CdTe the spectrum is not completely explained by the SO interaction. The JT effect can be incorporated by means of either interpretation B or interpretation C shown in Fig. 2. Since the former was already discussed in the previous section we begin the discussion with the latter. According to this interpretation[10] the line at 66.7 cm^{-1} would be due to an absorption from the ground state to the second excited states that transform according to the irreducible representation γ_4. We have not found a consistent way of making such an assignment. After the JT effect has been considered in first approximation, the ground state is a mixture of states $|(10)a\rangle$ and $|(31)a\rangle$ with a larger coefficient for the former one. In the same approximation the excited states under consideration would be mixture of states $|(41)w\rangle$, $|(40)w\rangle$, $|(42)w^a\rangle$, $|(42)w^b\rangle$, and $|(51)w\rangle$ and similar ones for states u and v. In both states the admixtures are of the same order of magnitude. This makes it difficult to understand why one can neglect the admixtures of states a while this is partially maintained for states w. When nothing is neglected the oscillator strength for such a transition comes out much weaker than the value reported by Vallin.[10] On the other hand, in order to make the assignment of interpretation C the energy of the first excited state w should decrease while the energy of the second excited state w should increase [see Fig. 1(c) of the Vallin article[11]]. This would occur if (and only if) the contributions from the states $|(42)w^a\rangle$ and $|(42)w^b\rangle$ are neglected. When nothing is neglected, the energy of the second excited state of symmetry w is also decreased.

In spite of these difficulties we performed complete first-order diagonalizations according to interpretation C. (We considered 5×5 matrices for states w, 4×4 matrices for states z, and 2×2 matrices for states a.) The SO parameter $|\lambda|$ was allowed to vary in the range from 85 to 100 cm^{-1}. The vibrational quantum $\hbar\omega$ that would cause the JT coupling was allowed to take values between 25 and 50 cm^{-1}. In each case the Jahn-Teller coupling constant K was varied seeking a good adjustment of the energy levels according to interpretation C. However, it was impossible to explain the low-temperature line at 66.7 cm^{-1} as well as the hot lines (interpretation B). The same procedure of diagonalization described above was used here. It was found that modes with vibrational ener-

TABLE IX. Functions and energies of the states of Fe^{2+} in CdTe after the Jahn-Teller effect has been considered. A final state is designated by a symbol according to the irreducible representation under which it transforms.

Irr. rep.	State	Final function in terms of zero-order vibronic eigenfunctions	Energy (cm^{-1})
γ_2'	$\lvert b'\rangle$	$0.7643\lvert(20)b\rangle - 0.6449\lvert(31)b\rangle$	100.3
γ_2	$\lvert b\rangle$	$0.6447\lvert(20)b\rangle + 0.7644\lvert(31)b\rangle$	91.7
γ_5'	$\lvert z'\rangle$	$0.6905\lvert(41)z\rangle + 0.7203\lvert(50)z\rangle - 0.0459\lvert(42)z\rangle + 0.0476\lvert(51)z\rangle$	72.9
γ_4	$\lvert w'\rangle$	$0.0569\lvert(40)w\rangle + 0.9945\lvert(41)w\rangle - 0.0303\lvert(51)w\rangle - 0.0601\lvert(42)w^a\rangle - 0.0565\lvert(42)w^b\rangle$	69.8
γ_5	$\lvert z\rangle$	$-0.7192\lvert(41)z\rangle + 0.6885\lvert(50)z\rangle + 0.0379\lvert(42)z\rangle + 0.0359\lvert(51)z\rangle$	66.9
γ_3'	$\lvert\theta'\rangle$	$0.9368\lvert(30)\theta\rangle + 0.3498\lvert(11)\theta\rangle$	52.3
γ_3	$\lvert\theta\rangle$	$-0.3499\lvert(30)\theta\rangle + 0.9368\lvert(11)\theta\rangle$	43.2
γ_4	$\lvert w\rangle$	$0.9978\lvert(40)w\rangle - 0.0587\lvert(41)w\rangle - 0.0293\lvert(51)w\rangle$	18.7
γ_1	$\lvert a\rangle$	$0.9990\lvert(10)a\rangle - 0.0446\lvert(31)a\rangle$	0.0

gy $\hbar\omega$ of about 49 cm^{-1} should be chosen as responsible for the Jahn-Teller coupling. For the values of the crystal-field and spin-orbit parameters given in Table VI we found that $\hbar\omega = 51$ and $E_{JT} = 0.17$ (both in cm^{-1}) give good agreement with the experiment. The results of this analysis are summarized in Table IX. If the absorptions at 36 and 49 cm^{-1} are due to local modes of the system as suggested in SRV,[9] the low-temperature spectrum of Fe^{2+} in CdTe is now simple to explain as will be done in the next section.

V. OSCILLATOR STRENGTHS

We will not develop here any theoretical aspect of oscillator strengths of transitions. This can be found in quantum-mechanics texts or in the already cited literature.[4,6,9]

For an electric dipole transition the oscillator strength between levels I and F can be expressed in the form

$$f_e(I,F) = \frac{2mE_{FI}}{\hbar^2 d_I} \sum_{i,f} \lvert\langle Ii\lvert R_z\lvert Ff\rangle\rvert^2 , \qquad (11)$$

while the oscillator strength for a magnetic dipole transition can be arranged in the form

$$f_m(I,F) = \frac{E_{FI}(n\,\epsilon/\epsilon_{\text{eff}})^2}{2\hbar^2 mc^2 d_I} \sum_{i,f} \lvert\langle Ii\lvert J_y\lvert Ff\rangle\rvert^2 . \qquad (12)$$

In this equation m represents the mass of the electron; $E_{FI} = E_F - E_I$ is the energy difference between the levels involved; d_I represents the degeneracy of the level occupied just before the transition occurs; the sum over i involves all the d_I states that are degenerate in level I, while the sum over f runs over all the states that are degenerate in level F. The speed of light is represented by the usual symbol c; n represents the refraction index of the substance, and $\epsilon/\epsilon_{\text{eff}}$ is the ratio of the average electric field in the

crystal to the effective electric field at the location of the Fe^{2+} ion.

For simplicity we have chosen electromagnetic radiation propagating in the direction of the positive x axis and polarized in the direction of the z axis. Electric dipole matrix elements involve $R_z = \sum_i \vec{r}_i \cdot \hat{z}$, where $\vec{r}_i$ is the position vector of the ith electron and $\hat{z}$ is a unit vector in the direction of the z axis. The matrix element $\langle Ii\lvert R_z\lvert Ff\rangle$ vanishes when the mixing due to SO interaction is neglected. When this mixing is considered, matrix elements between orbital states have been guessed[4] to be about 0.1 Å unless they vanish.

In the matrix element $\langle Ii\lvert J_y\lvert Ff\rangle$, the angular momentum operator can be taken as the spin operator since the orbital angular momentum contribution to the magnetic moment can be neglected. Matrix elements between spin states have a value $2\hbar$, unless they vanish.

For cubic crystals the ratio $\epsilon/\epsilon_{\text{eff}}$ is given in a rough approximation[22] by the Lorentz local-field ratio, namely,

$$\epsilon_{\text{eff}}/\epsilon = \frac{1}{3}(n^2 + 2) , \qquad (13)$$

where n is the far-infrared refraction index of the substance. The experimental values for n^2 in CdTe (Refs. 23 and 24) and ZnS (Ref. 25) are 9.7 and 8.3, respectively.

For ZnS:Fe^{2+} the electric and magnetic dipole transitions are illustrated in Figs. 3(a) and 3(b), respectively. The experimental line at 14.6 cm^{-1} corresponds to a 1−2 magnetic dipole transition $(\gamma_1 \rightarrow \gamma_4)$. The intense line at 45.1 cm^{-1} corresponds to a 1−4 $(\gamma_1 \rightarrow \gamma_5)$ electric-dipole transition. As for the hot lines, we see that the line 2−3 (3−4 and 4−5 also) is masked by the 1−2 transition. Something similar happens with the 2−5 line which is masked by the 1−4 transition. This is a consequence of the ap-
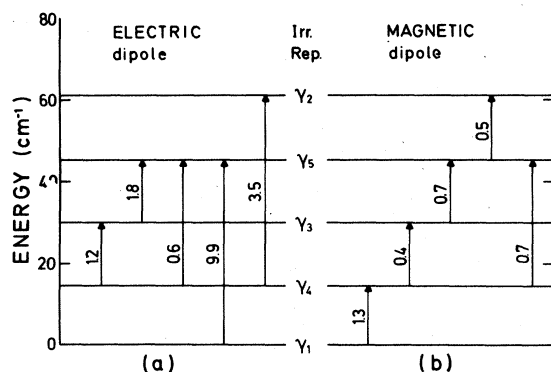
FIG. 3. Oscillator strengths in units of 10^{-8} for absorptions of electromagnetic radiations within states of the lower electronic multiplet of Fe^{2+} in ZnS ($|\langle Ii|R_z|Ff\rangle| = 0.1$ Å; $n\epsilon_{eff}/\epsilon = 9.9$).

proximate equal spacing between successive levels. So we are left with the 2—4 transition as the only additional one to be observed at high temperatures; this is the hot line at 45.3 cm^{-1}.

For Fe^{2+} in CdTe the analysis is not obvious. The electric and magnetic dipole transitions are illustrated in Figs. 4(a) and 4(b), respectively. (Since the low-temperature spectrum over 80 cm^{-1} is very complicated we will only study those levels with energy less than 80 cm^{-1}.) Three low-temperature lines are clearly predicted. The magnetic dipole transition $\gamma_1 \rightarrow \gamma_4$ explains the experimental absorption at 18.6 cm^{-1}. The splitting of the electric dipole line into a $\gamma_1 \rightarrow \gamma_5$ and $\gamma_1 \rightarrow \gamma'_5$ transition explains the experimental lines at 66.7 and 73.2 cm^{-1}, respectively. The high-temperature line at 54.8 cm^{-1} is explained by a $\gamma_4 \rightarrow \gamma'_5$ transition. We also obtain a hot line at about 34 cm^{-1} which is shown in the spectrum as a slight bump in the high-temperature spectrum around 36
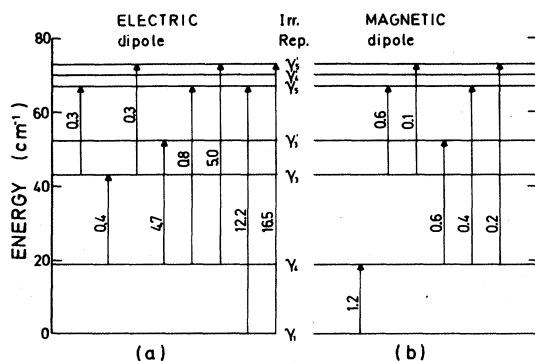

FIG. 4. (a),(b) Oscillator strengths in units of 10^{-8} for absorptions of electromagnetic radiation within states of the lower electronic multiplet of Fe^{2+} in CdTe. Vibronic functions are used. Oscillator strengths under 10^{-9} are not included ($|\langle Ii|R_z|Ff\rangle| = 0.1$ Å; $n\epsilon_{eff}/\epsilon = 12.1$).

cm^{-1}.[9] The rest of the allowed transitions are much weaker and would be difficult to identify in the experimental results.

VI. CONCLUSIONS

Several conclusions can be drawn from the results above.

The values of D (effective $|Dq|$) are smaller than the experimental values both for CdTe:Fe^{2+} and ZnS:Fe^{2+}. The experimental values were obtained in a way that the JT effect can be neglected. Then, it is reasonable to assume that this effect causes the quenching of the splitting of the two multiplets. Average JT energies for the upper multiplet have been estimated to be 535 cm^{-1} for ZnS and 255 for CdTe.[4] This implies a larger quenching for ZnS than for CdTe. The first of the ratios in Eqs. (4) and (5) verifies this property in a qualitative way. Since the vibrational modes that couple to the electronic states of the upper multiplet are not known, a quantitative analysis is not possible at the moment.

The values of x (absolute value of the SO interaction for matrix elements connecting the upper and the lower multiplets) are smaller than the theoretical value for both CdTe:Fe^{2+} and ZnS:Fe^{2+}. Such a value[16] corresponds to the free ion, so the JT effect was not considered. The role of this effect in the quenching of the SO interaction is clear from the second of the ratios in Eqs. (4) and (5). The reduction of the spin-orbit parameter is more pronounced for ZnS than for CdTe in accordance with their respective JT energies. This effect would be even more pronounced if the spin-spin interaction (which is not quenched) could be separated out. The reduction of the SO interaction in the upper multiplet is large. Again, we lack knowledge of the actual JT coupling to achieve a quantitative analysis. However, the phenomenological treatment gives good results. The reduction is larger for ZnS than for CdTe according to the values of R_a in Eqs. (4) and (5). This can also be understood from the point of view of the relative sizes of the atoms. The ionic radius[26] of Fe^{2+} (0.76 Å) is very similar to the ionic radius of Zn^{2+} (0.83 Å). This means that the substituted ion is well trapped among its neighbors and the JT coupling should be relatively important. The ionic radius of Cd^{2+} (1.03 Å) is larger than the radius of the substituted ion. The Fe^{2+} ion in CdTe is not well trapped among the neighbors so the JT coupling is less important than that in ZnS.

The JT effect for the states of the lower multiplet is negligible in most cases. The orbital electronic states belong to the E representation and the coupling seems to be rather weak. However, an interesting phenomenon occurs when the vibrational quantum corresponding to the Jahn-Teller phonons possess an

energy very close to the energy difference between electronic states. In this case vibronic states that differ in one vibrational quantum are degenerate. In such cases even a weak JT coupling can cause modifications to the vibronic spectra. In ZnS the spectrum shows no evidence of this effect.

The oscillator strengths that were calculated in the previous section agree well with the experimental determinations. The agreement is within a factor of 2 or 3 due to the approximations that were introduced. The electric dipole oscillator strengths are uncertain due to the estimate of the matrix element of the sort $|\langle Ii|R_z|Ff\rangle|$. When values less than 0.1 Å are tried for this integral better adjustment is obtained for the electric oscillator strengths. The magnetic oscillator strengths are uncertain by the ratio ϵ_{eff}/ϵ, since Eq. (13) is a very rough approximation.

It would be desirable to determine the spectroscopic properties of several magnetic impurities in all of the II—VI compounds in order to get a better understanding of these effects. Independent experiments based on neutron scattering would give a definite proof on the existence of one or two lines due to magnetic dipole transitions. It would be also desirable to know the information that polarized absorption spectra in the far infrared can provide for Fe^{2+} in ZnS and CdTe. None of the above experiments is known to the authors.

ACKNOWLEDGMENTS

---

*Currently at Max-Planck-Institut für Festkörperforschung, Federal Republic of Germany.

[1]H. A. Jahn and E. Teller, Proc. R. Soc. London Ser. A 161, 220 (1937); R. Englman, The Jahn-Teller Effect in Molecules and Crystals (Wiley-Interscience, New York, 1972).

[2]N. Vagelatos, D. Wehe, and J. S. King, J. Chem. Phys. 60, 3613 (1974).

[3]J. M. Rowe, R. M. Nicklow, D. L. Price, and K. Zanio, Phys. Rev. B 10, 671 (1974).

[4]G. A. Slack, F. S. Ham, and R. M. Chrenko, Phys. Rev. 152, 376 (1966).

[5]F. S. Ham and G. A. Slack, Phys. Rev. B 4, 777 (1971).

[6]G. A. Slack, S. Roberts, and F. S. Ham, Phys. Rev. 155, 170 (1967).

[7]J. T. Vallin, G. A. Slack, and C. C. Bradley, Phys. Rev. B 2, 4406 (1970).

[8]F. W. Sheard, T. F. Smith, G. K. White, and J. A. Birch, J. Phys. C 10, 645 (1977).

[9]G. A. Slack, S. Roberts, and J. T. Vallin, Phys. Rev. 187, 511 (1969).

[10]J. T. Vallin, Phys. Rev. B 2, 2390 (1970).

[11]G. A. Slack, Phys. Rev. B 6, 3791 (1972).

[12]G. Spavieri and E. E. Vogel, Nuovo Cimento Lett. 19, 251 (1977).

[13]M. T. Hutchings, in Solid State Physics, edited by F. Seitz and D. Turnbull (Academic, New York, 1964), Vol. 16, p. 227.

[14]A. R. Edmonds, Angular Momentum in Quantum Mechanics (Princeton University Press, Princeton, New Jersey, 1960).

[15]In order to identify the states of the different representations we adopt the following notation: $|a\rangle$ for state of γ_1; $|b\rangle$ for state of γ_2; $|\Theta\rangle$ and $|\epsilon\rangle$ for states of γ_3; $|u\rangle$,

$|v\rangle$, and $|w\rangle$ for states of γ_4; $|x\rangle$, $|y\rangle$, and $|z\rangle$ for states of γ_5. Lower case letters are used for states of the lower multiplet, while capital letters are used for states of the upper multiplet. Primes are introduced whenever there is ambiguity. When referring to symmetry properties not attached to any multiplet, in particular, we use the notation A_1, A_2, E, T_1, and T_2 to design the representations of T_d. The same notation is used for vibrations.

[16]C. E. Moore, Atomic Energy Levels (U.S. GPO, Washington, D.C., 1952), Vol. 2, p. 60.

[17]G. F. Koster, J. O. Dimmock, R. G. Wheeler, and H. Statz, Properties of the Thirty-Two Point Groups (MIT University Press, Cambridge, Mass., 1963).

[18]R. E. Watson and M. Blume, Phys. Rev. 139, A1209 (1965).

[19]M. D. Sturge, in Solid State Physics, edited by F. Seitz, D. Turnbull, and H. Ehrenreich (Academic, New York, 1967), Vol. 20, p. 91.

[20]E. Merzbacher, Quantum Mechanics (Wiley, New York, 1961).

[21]E. E. Vogel, Ph.D. thesis (John Hopkins University, 1975) (unpublished).

[22]D. L. Dexter, in Solid State Physics, edited by F. Seitz and D. Turnbull (Academic, New York, 1959), Vol. 6, p. 353.

[23]D. Berlincourt, H. Jaffe, and L. R. Shiozawa, Phys. Rev. 129, 1009 (1963).

[24]B. Segall, M. R. Lorentz, and R. E. Halsted, Phys. Rev. 129, 2472 (1963).

[25]The refractive index of ZS has been determined in several experiments yielding approximately the same results. We use here the value chosen in Ref. 6.

[26]C. Kittel, Introduction to Solid State Physics, 4th ed. (Wiley, New York, 1974), p. 129.